Inorganic Chemistry

ARTICLE

pubs.acs.org/IC

First Three-Dimensional Inorganic−Organic Hybrid Material Constructed From an "Inverted Keggin" Polyoxometalate and a Copper(I)-Organic Complex

Bo Liu,[†,§] Zhen-Tao Yu,[‡] Jin Yang,*[,†] Wu Hua,[†] Ying-Ying Liu,[†] and Jian-Fang Ma*[,†]

[†]Key Laboratory of Polyoxometalate Science, Department of Chemistry, Northeast Normal University, Changchun 130024, People's Republic of China

[‡]Eco-Materials and Renewable Energy Research Center, National Laboratory of Solid State Microstructures, Nanjing University, Nanjing 210093, People's Republic of China

[§]Department of Chemistry, Jilin Normal University, Siping 136000, People's Republic of China

Supporting Information

ABSTRACT: A new polyoxometalate (POM) based on a flexible bidentate ligand and "inverted Keggin" inorganic building block, namely, $[Cu_8L_8[Mo_{12}O_{46}(AsPh)_4]_2]\cdot H_2O$ (**1**), where L is 1,3-bis(1,2,4-triazol-1-yl)propane, has been synthesized under hydrothermal condition. In **1**, the "inverted Keggin" $[Mo_{12}O_{46}(AsPh)_4]^{4-}$ building blocks are linked by the one-dimensional (1D) zigzag $[Cu^I(trans\text{-}L)]^+$ chains and $[Cu^I_4(cis\text{-}L)_4]^{4+}$ macrocycles to yield a three-dimensional (3D) framework. The compound **1** represents the first 3D "inverted Keggin" polyoxometalate modified by a transition-metal complex. Topologically, the 3D framework can be considered as an 8-connected net with a Schläfli symbol of $4^{22}\cdot 6^6$. As far as we know, compound **1** is the highest-connected uninodal network topology presently known for POM-based materials. The compound was characterized by its IR spectrum, UV−vis spectrum, thermogravimetric analysis (TGA), and powder X-ray diffraction (XRD) patterns. Remarkably, compound **1** exhibits photocatalytic activity for dye degradation under visible light irradiation and shows good stability toward visible-light photocatalysis.

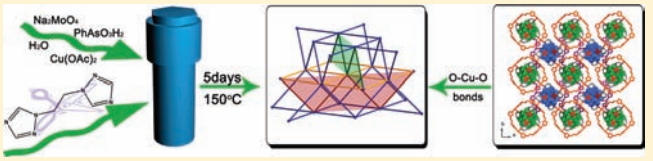

INTRODUCTION

The design and synthesis of inorganic−organic hybrid materials based on polyoxometalates (POMs) are of great interest not only for their potential applications in catalysis, medicine, and nanotechnology but also for their intriguing variety of architectures and fascinating topologies.[1] As we know, the most effective approach to fabricate such materials is the modification of POMs by transition-metal complexes (TMCs).[2] So far, a variety of appealing high-dimensional materials constructed from classical POMs, such as Keggin-,[3] Wells−Dawson-,[4] and Anderson-type[5] POMs, have been reported.

Clusters with type of $[Mo_{12}O_{46}(AsR)_4]^{4-}$ (R = CH_3, C_2H_4OH, C_6H_5, p-$C_6H_4NH_3$, p-C_6H_4CN) were first prepared by Debray[6] and Rosenheim and Traube.[7] Subsequently, these clusters were named as "inverted Keggin" POMs for the first time by Pope and Sasaki.[8,9] Different from the traditional Keggin configuration, the heteroatoms of the "inverted Keggin" are located on the surface of the structure, as opposed to the interior. Compared with the aforementioned TMCs-modified classical POMs, the hybrid materials based on "inverted Keggin" type POMs have been far less explored because of their steric hindrance and the choice of inappropriate organic ligand. Thus far, only a few such hybrids have been reported.[10,11] In particular, they are mainly focused on zero-dimensional (0D) and two-dimensional (2D) structures modified by 2,2′-bipyridine and its derivative.[10] Zubieta and coworkers reported two 0D "inverted Keggin" hybrids for the first time.[10a] Soon afterward, two 2D hybrids were obtained by Stein and Zubieta, respectively.[10b,11] However, the three-dimensional (3D) TMCs-modified "inverted Keggin" POMs have never been observed to date.

When the bulk aromatic chelating ligands, such as 2,2′-bipyridine and 1,10-phenanthroline, were utilized to build the TMCs-modified "inverted Keggin" type POMs, the steric hindrance at the metal centers should have increased. Obviously, the steric hindrance will reduce the final dimensions of networks.[12] To overcome this difficulty, our synthetic strategy is to select an appropriate organic ligand which possesses bridging mode and high flexibility, and then utilizes an "inverted Keggin" POM as an inorganic building block to construct a 3D high-connected framework. In this regard, 1,3-bis(1,2,4-triazol-1-yl)propane (L) has good flexibility and conformational freedom, which allows it to conform to the coordination environments of the metal ions and POMs.

In this work, two new POMs based on flexible bidentate ligands and an "inverted Keggin" inorganic building block, namely,

Received: May 27, 2011
Published: August 15, 2011

Table 1. Crystal Data and Structure Refinement for Compound 1

empirical formula	$C_{104}H_{122}As_8Cu_8Mo_{24}N_{48}O_{93}$
Fw	6942.74
crystal size [mm]	0.31 × 0.28 × 0.17
crystal system	tetragonal
space group	$I4(1)/a$
a [Å]	20.7511(2)
c [Å]	43.0804(15)
volume [Å^3]	18550.8(7)
Z	4
D_c(g/cm^3)	2.486
GOF	1.074
reflns collected/unique	41970/11310
R_{int}	0.0510
$R1$ [$I > 2\sigma(I)$]	0.0522
$wR2$ (all data)	0.1244

$[Cu_8L_8[Mo_{12}O_{46}(AsPh)_4]_2]\cdot H_2O$ (**1**) and $[Cu^I_4(cis\text{-}L')_4(H_2O)_4]$-$[Mo_{12}O_{46}(AsPh)_4]\cdot 2H_2O$ (**2**), where L′ is 1,2-bis(1,2,4-triazol-1-yl)ethane, have been synthesized under hydrothermal condition. Remarkably, compound **1** represents the first 3D example of TMCs-modified "inverted Keggin" POMs.

EXPERIMENTAL SECTION

Materials and Instruments. The organic ligands (L and L′) were synthesized by the general method described in the literature.[13] Other reagents were purchased from commercial sources and used as received. Elemental analysis (C, H, and N) were conducted on a Perkin-Elmer 2400CHN elemental analyzer. The inductively coupled plasma (ICP) analysis was performed on a Leeman Laboratories Prodigy inductively coupled plasma-optical atomic emission spectrometer (ICP-AES). The FT-IR spectrum was recorded from KBr pellet in the range 4000−400 cm^{-1} on a Mattson Alpha-Centauri spectrometer. The solid diffuse reflectance UV−vis spectrum was recorded on a Varian Cary 500 UV−vis spectrometer, whereas the UV−vis spectra for solution samples were obtained on a Shimadzu UV 2450 spectrometer. The powder X-ray diffraction (PXRD) data was collected on a Rigaku RINT2000 diffractometer at room temperature with Cu K_α radiation. Thermogravimetric analysis (TGA) was performed on a Perkin-Elmer TG-7 analyzer heated from room temperature to 600 °C under nitrogen gas. Photocatalytic experiments in aqueous solutions were carried out in a 500 mL water-cooled quartz cylindrical vessel. The reaction mixture in the vessel was maintained at room temperature by a continuous flow of water through an external cooling coil. The visible light source was a 500 W Xe lamp (main output >400 nm). To establish an adsorption/desorption equilibrium of methylene blue (**MB**) on the sample surface, a suspension of powdered catalyst (70 mg) in fresh aqueous solution of **MB** (200 mL, 1.0 × 10^{-5} mol L^{-1}) was magnetically stirred in the dark for at least 30 min in the vessel before irradiation. At given irradiation time intervals, a series of aqueous solutions of a certain volume were collected and separated through centrifuge to remove suspended catalyst particles and then subjected to spectroscopic measurement on the UV−vis spectrometer. The organic dye concentration was estimated by the absorbance at 665 nm, which directly relates to the structure change of its chromophore.

X-ray Crystallography. Single-crystal X-ray diffraction data for **1** and **2** were recorded on an Oxford Diffraction Gemini R CCD with graphite-monochromated Mo Kα radiation (λ = 0.71073 Å) at 298 K. The structure was solved by the Direct Method of SHELXS-97[14] and refined by full-matrix least-squares techniques using the SHELXL-97 program[15] within WINGX.[16] Non-hydrogen atoms were refined with anisotropic temperature parameters, and hydrogen atoms of the ligands were refined as rigid groups. The hydrogen atoms associated with the water molecules were not located from the difference Fourier maps. The detailed crystallographic data and structure refinement parameters for **1** and **2** are summarized in Table 1 and Supporting Information, Table S1, respectively.

Synthesis of $[Cu_8L_8[Mo_{12}O_{46}(AsPh)_4]_2]\cdot H_2O$ 1. A mixture of $Cu(OAc)_2\cdot H_2O$ (100 mg, 0.5 mmol), L (90 mg, 0.5 mmol), $Na_2MoO_4\cdot 2H_2O$ (242 mg, 1 mmol), $PhAsO_3H_2$ (200 mg, 1 mol), and water (10 mL) was placed in an 18 mL Teflon reactor, the pH value was adjusted to about 2 by 4 M HCl, and kept under autogenous pressure at 150 °C for 5 days. Then the mixture was cooled to room temperature, and brown crystals of **1** were obtained in a 36% yield based on Cu. Elemental analysis results for $C_{104}H_{122}As_8Cu_8Mo_{24}N_{48}O_{93}$: Calcd (%): C 17.99, H 1.77, N 9.68, Cu 7.32, Mo 33.17; Found (%): C 17.85, H 1.68, N 9.73, Cu 7.37, Mo 33.23. FTIR (KBr pellet, cm^{-1}): 3445(s), 3120(s), 3049(s), 1536(s), 1440(s), 1281(m), 1212(s), 1135(m), 1087(s), 949(m), 918(m), 867(s), 672(m), 587(s), 489(m).

Synthesis of $[Cu^I_4(cis\text{-}L')_4(H_2O)_4][Mo_{12}O_{46}(AsPh)_4]\cdot 2H_2O$ 2. Compound **2** was prepared similarly to that of compound **1**, but the L′ (L′ = 1,2-bis(1,2,4-triazol-1-yl)ethane) (82 mg, 0.5 mmol) was used instead of L. Brown crystals of **2** were obtained in a 42% yield based on Cu. Elemental analysis results for $C_{48}H_{64}As_4Cu_4Mo_{12}N_{24}O_{52}$: Calcd (%): C 16.40, H 1.84, N 9.57; Found (%): C 16.45, H 1.77, N 9.49.

RESULTS AND DISCUSSION

Synthesis. The redox reaction from Cu^{II} to Cu^I can easily occur under hydrothermal condition, and is highly pH dependent.[17] For the preparation of compound **1**, the reaction pH value of the solution is very important. Detailed experiments show that compound **1** can not be obtained when the pH value is lower than 1.8 or higher than 2.2. The final pH range is about 2.2−2.5 at the end of the hydrothermal treatment. In addition, we have tried to replace $Cu(OAc)_2\cdot H_2O$ with $Co(OAc)_2\cdot 4H_2O$ or $NiCl_2\cdot 6H_2O$ in the same reaction conditions, but we can not obtain its crystal samples. In other words, the Cu^I position in **1** can not be replaced by other metals. It is apparent that the existence of the Cu^I is essential in the lattice of **1**. It is well established that at high temperature both the solvent and the N-donor ligand may serve as effective reducing agents for Cu^{II} to Cu^I, and hence to generate Cu^I-containing compounds.[17c]

Description of Structure. Single-crystal X-ray analysis reveals that **1** crystallizes in the tetragonal space group $I4_1/a$. The asymmetric unit of **1** contains two Cu^+ cations, two L ligands (*cis*-L and *trans*-L) (Supporting Information, Figure S1), two crystallographically unique quarters of $[Mo_{12}O_{46}(AsPh)_4]^{4-}$ polyoxoanions, and one-quarter of an uncoordinated water molecule (Supporting Information, Figure S2). Both Cu1 and Cu2 are coordinated by two nitrogen atoms from two L ligands and two terminal oxygen atoms from two $[Mo_{12}O_{46}(AsPh)_4]^{4-}$ polyoxoanions (Figure 1). The Cu−O distances vary from 2.53(8) to 2.77(6) Å, and the Cu−N distances range from 1.84(7) to 1.88(9) Å (Table 2). The bond valence sum calculations[18] confirm that all Mo centers are in +VI oxidation states, all the As centers are in +V oxidation state, and the Cu centers are in +I oxidation state. The Cu−O, As−O, and Mo−O lengths are in the normal ranges.[8−11,19]

As shown in Figure 2, Cu1 cation connects neighboring *trans*-L ligands to form a 1D zigzag $[Cu^I(trans\text{-}L)]^+$ chain (motif **I**). Cu2 and its three symmetry-related cations are bridged by four *cis*-L ligands to yield a $[Cu^I_4(cis\text{-}L)_4]^{4+}$ macrocycle (motif **II**).

dx.doi.org/10.1021/ic201135g |*Inorg. Chem.* 2011, 50, 8967–8972

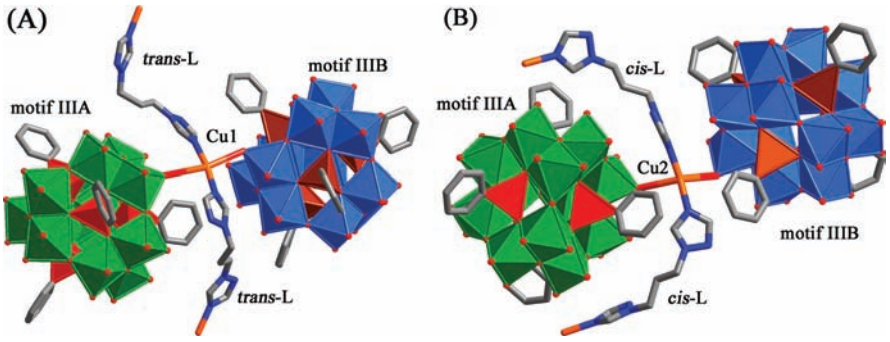

Figure 1. Coordination environments of Cu^{+} cations: (A) *trans*-L ligands and polyanions; (B) *cis*-L ligands and polyanions.

Table 2. Selected Bond Lengths [Å] and Angles [deg] for 1[a]

Cu(1)−N(1)	1.847(10)	Cu(2)−O(10)$^{\#5}$	2.665(1)
Cu(1)−N(6)$^{\#1}$	1.889(9)	Cu(2)−O(18)$^{\#6}$	2.538(3)
Cu(2)−N(7)	1.877(8)	Cu(2)−N(12)$^{\#2}$	1.881(7)
Cu(1)−O(3)$^{\#3}$	2.760(9)	Cu(1)−O(21)$^{\#4}$	2.775(6)
N(1)−Cu(1)−N(6)$^{\#1}$	171.0(5)	N(7)−Cu(2)−N(12)$^{\#2}$	172.6(3)
O3$^{\#3}$−Cu1-O21$^{\#4}$	161.3(4)	O10$^{\#5}$−Cu2-O18$^{\#6}$	119.5(3)

[a] Symmetry transformations used to generate equivalent atoms: $^{\#1}x$, $y+1/2$, $-z+1$; $^{\#2}y-1/4$, $-x+5/4$, $-z+5/4$; $^{\#3}-x+1$, $-y+1$, $-z+1$; $^{\#4}y-1/4$, $-x+3/4$, $z-1/4$; $^{\#5}y+1/4$, $-x+5/4$, $z+1/4$; $^{\#6}-x$, $-y+3/2$, z.

The building block $[Mo_{12}O_{46}(AsPh)_4]^{4-}$ (motif **III**) exhibits "inverted Keggin" configuration which consists of four $[PhAsO_3]$ tetrahedra and four $[Mo_3O_{12}]$ subunits of *cis*-edge sharing $[MoO_6]$ octahedra. It has tetrahedral symmetry, but the heteroatoms are located on the outer surface of the cluster as opposed to the interior (Figure 3).

Notably, there are two kinds of crystallographically unique motifs **III**, namely, **IIIA** and **IIIB**. The motif **IIIA** is located in the macrocycle motif **II**. The Cu2−O10 and its three symmetry-related bonds between motifs **IIIA** and **II** result in an interesting $[Cu_4(cis\text{-}L)_4][Mo_{12}O_{46}(AsPh)_4]$ subunit (Figure 4). If motif **II** is considered as a satellite running track, then, four Cu2 cations follow the polyoxoanion like a satellite (Figure 4). Next, the motifs **IIIB** link two motifs **I** through symmetry-related Cu1−O21 bonds to form a 1D ladder-like inorganic−organic hybrid chain (Figure 5a). Further, each motif **IIIB** in the 1D ladder-like hybrid chain joins four $[Cu_4(cis\text{-}L)_4][Mo_{12}O_{46}(AsPh)_4]$ subunits through symmetry-related Cu2−O18 bonds to yield a 2D inorganic−organic hybrid layer in the *ab* plane (Figure 5b). In the 2D hybrid layer, the ladder-like chains are parallel to each other. Remarkably, if all *cis*-L ligands and motifs **I** are removed from the 2D hybrid layer, the layer structure can be considered as a 4-connected (4,4) network constructed by motifs **IIIA**, **IIIB** and Cu2 cations (Supporting Information, Figure S3).

Finally, neighboring hybrid layers shared Cu1 cations through the terminal O atoms (O3 and O21) to yield a 3D framework of **1** (Supporting Information, Figures S4 and S5). Each motif **IIIA** connects eight nearest motifs **IIIB** by O−Cu−O bonds, and each motif **IIIB** also connects eight nearest motifs **IIIA** (Supporting Information, Figure S6). From a topological viewpoint, the 3D structure can be considered as an 8-connected framework with a Schläfli symbol of $4^{22}\cdot6^6$ (Supporting Information, Figure S7). As far as we know, compound **1** represents the highest-connected uninodal network topology presently known for POM-based materials.

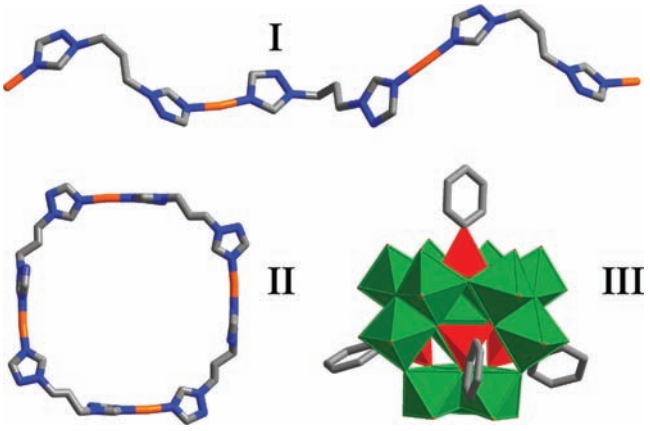

Figure 2. View of three different motifs in **1**: (**I**) 1D $[Cu^{I}(trans\text{-}L)]^{+}$ chain, (**II**) 0D $[Cu^{I}_4(cis\text{-}L)_4]^{4+}$ macrocycle, and (**III**) "inverted Keggin" cluster $[Mo_{12}O_{46}(AsPh)_4]^{4-}$.

Significantly, the structure of **1** is different from that of the familiar body-centered cubic lattice (bcu).[20] As shown in Supporting Information, Figure S8, the parallel (4,4) nets (orange) of both bcu and **1** are cross-linked by zigzag chains (green and dark red), however, the detailed connection modes are different. In bcu net, the green and dark red zigzag chains are in the same plane and bridge across the same diagonal of the (4,4) net (Supporting Information, Figure S8a). In **1**, however, they are in the decussate plane and bridge across the different diagonal of the (4,4) net (Supporting Information, Figure S8b).

Optical Band Gap. According to previous literature, several POM-based inorganic−organic hybrid compounds have been reported to be promising semiconductors.[21] Therefore, the UV−vis diffuse reflectance spectrum of **1** was measured to achieve its band gap (E_g) (photoresponse wavelength region). The E_g was confirmed as the intersection point between the energy axis and the line extrapolated from the linear portion of the adsorption edge in a plot of the Kubelka−Munk function F against E.[22] The optical absorption associated with E_g can be assessed at 1.72 eV for **1** (Figure 6), which illustrates the presence of an optical band gap and the nature of semiconductivity for **1**.[21b] Therefore, compound **1** possesses possible potential for visible-light photocatalytic activity.[23]

It is helpful to identify the main characteristic of the optical band gap showed above using Density Functional Theory (DFT) calculations. We consider a simplified structure based on the crystal data with $[Cu_4(cis\text{-}L)_4][Mo_{12}O_{46}(AsPh)_4]$ subunit (Supporting

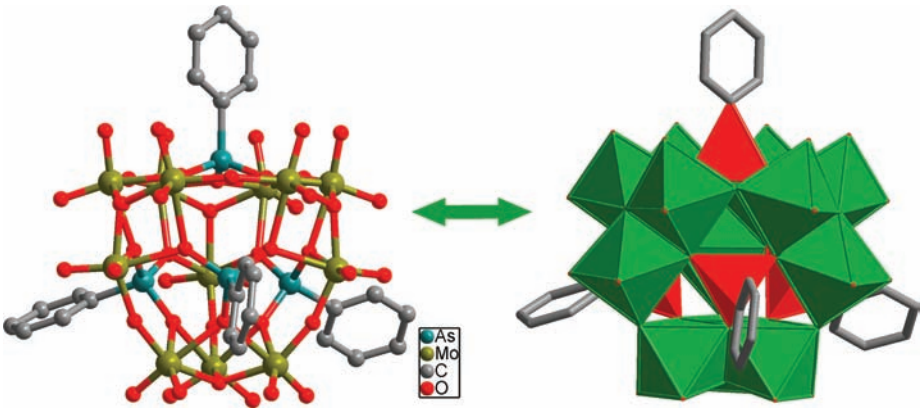

Figure 3. Ball-stick and polyhedron representations of the "inverted Keggin" type POM.

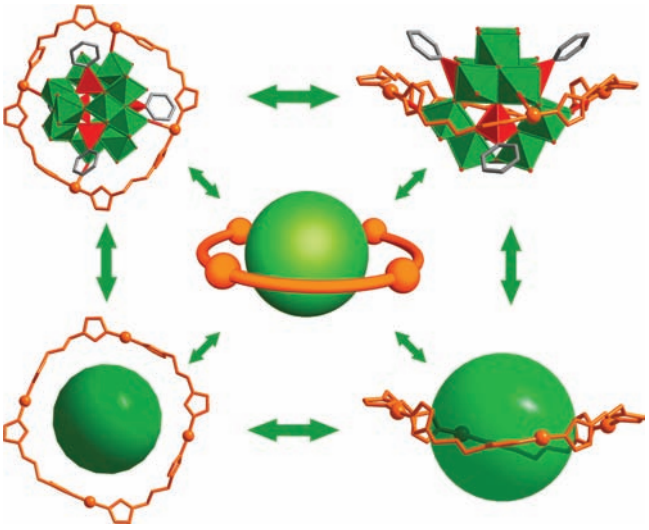

Figure 4. View of $[Cu_4(cis\text{-}L)_4][Mo_{12}O_{46}(AsPh)_4]$ subunit formed by motifs **II** and **IIIA**.

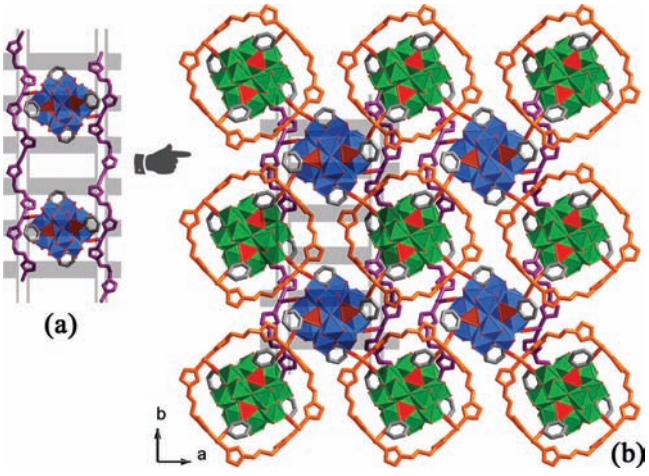

Figure 5. (a) 1D ladder-like hybrid chains and (b) view of the 2D inorganic–organic hybrid layer formed by $[Cu_4(cis\text{-}L)_4][Mo_{12}O_{46}(AsPh)_4]$ subunits and 1D ladder-like hybrid chains.

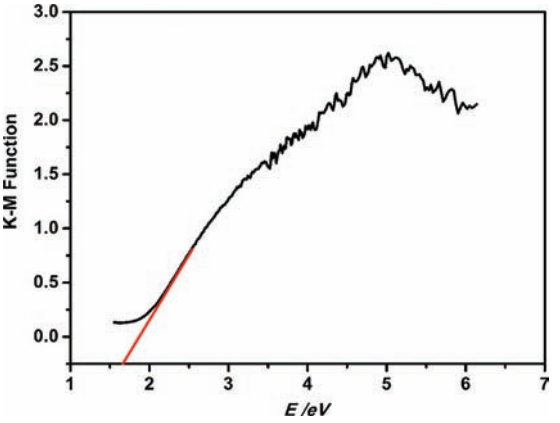

Figure 6. Kubelka–Munk-transformed diffuse reflectance spectrum of **1**.

Information, Figure S9) to perform the DFT calculation. We use the B3LYP functional in conjunction with 6-31G(d) for O, As, N, C, H and Lanl2dz for Cu and Mo. The model we adopt has S_4 symmetry. The calculation is performed with the Gaussian 09 program.[24] The highest occupied molecular orbital (HOMO) and the lowest unoccupied molecular orbital (LUMO) of the model are shown in the Supporting Information, Figure S9. The main constituent of the LUMO mainly distributes among the metal molybdenum and bridging oxygen, while the HOMO is mainly the terminal oxygen and copper. We conclude that the POM component should be responsible for its optical band gap. This is in accordance with the fact that Mo in the POM has the d^0 electron configuration. On the basis of the ground state property, we predicted in theory that the electronic transitions can be assigned to the oxygen-to-metal (O→Mo ligand-to-metal transfer [LMCT]).[2g]

Photocatalysis Property. Photocatalytic activity is an attractive property of POMs.[25−27] In the process of photocatalytic degradation by POMs, the organic dye chromophore is damaged and broken down into nonpolluting small molecules. Herein, methylene blue (**MB**), as a model of dye contaminant, was selected for evaluating the activity of photocatalysts in the purification of wastewater. The experiment with a typical process, a suspension containing **1** (70 mg) and a 200 mL **MB** (1.0×10^{-5} mol L^{-1}) solution was stirred in the dark for about 30 min. It was then stirred continuously under xenon-lamp irradiation. Every 30 min, 3 mL of samples were taken out of the reactor for

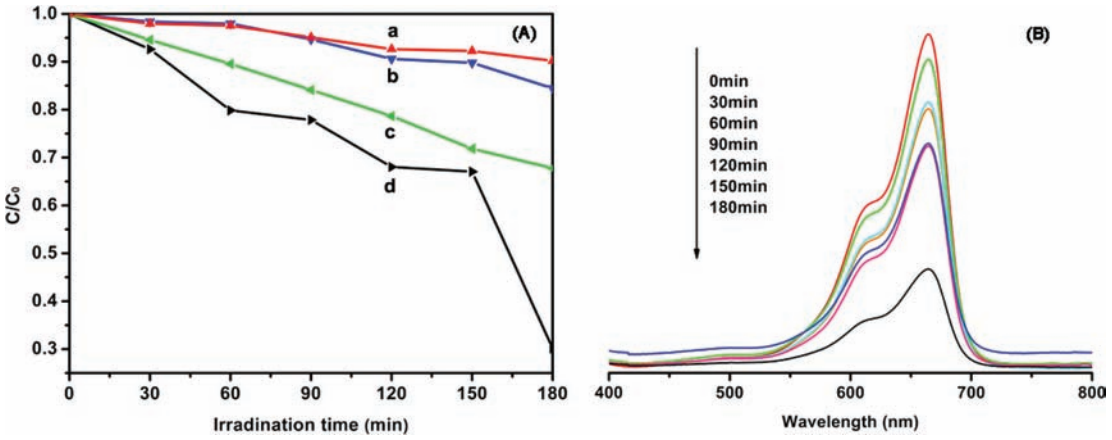

Figure 7. (A) Plots of concentration versus irradiation time for (a) **MB** under Xe lamp irradiation without photocatalyst, (b) **MB** under Xe lamp irradiation in the presence of **1** under the N_2 condition, (c) **MB** under Xe lamp irradiation in the presence of **2** and (d) **MB** under Xe lamp irradiation in the presence of **1**, and (B) UV−vis absorption spectra of the **MB** solution during the decomposition reaction under visible light irradiation in the presence of **1**.

analysis. As illustrated in Figure 7, the concentration of **MB** versus reaction time of **1** was plotted. It can be seen that the photocatalytic activity increases from 10% (without any catalyst) to 70% for **1** after 3 h of irradiation (Figure 7). By contrast, the new 0D compound $[Cu^{I}_4(cis\text{-}L')_4(H_2O)_4][Mo_{12}O_{46}(AsPh)_4]\cdot 2H_2O$ **2** (see Supporting Information) only enables the decomposition of 33% of the **MB** after 3 h of irradiation (Figure 7). These results suggest that the more extended framework of **1** has an advantage over the 0D compound **2** during the photocatalytic decomposition reaction with **MB**.[25] To study the impact of oxygen on the photocatalytic degradation reaction of **1**, the photocatalytic experiment without the O_2 was carried out under the same condition. The photocatalytic activity increases from 10% (without any catalyst) only to 16% for **1** after 3 h of irradiation under the N_2 condition (Figure 7). Clearly, the presence of O_2 was proven to be essential for the photocatalytic activity of **1**. It should be pointed out that the photocatalytic properties for POMs in aqueous solutions have been well documented in the literature, whereas there have been very few reports about photocatalysis of POMs modified by TMCs.[25]

As we know, the **MB** itself is stable to O_2 and visible light. Once associated with photoexcited $[Mo_{12}O_{46}(AsPh)_4]^{4-}$ species, the degradation of **MB** starts and generates active intermediates, which are further cracked by the oxygen-centered species in the solution, ending up with small organic acids and CO_2.[28]

After photocatalysis, the color of sample **1** remains unchanged. In addition, the photostability of compound **1** was monitored by using powder XRD patterns during the course of photocatalytic reactions (Supporting Information, Figure S10). The powder XRD pattern is nearly identical to that of the original compound implying that **1** maintains its structural integrity after photocatalysis reaction, which confirmed that its stability toward photocatalysis is good.

CONCLUSION

In conclusion, a 3D inorganic−organic hybrid material based on an "inverted Keggin" building block has been successfully synthesized and characterized. The compound **1** represents the first 3D TMCs-modified "inverted Keggin" POM. The result indicates that the flexible bis(triazole) ligand is a good candidate for the construction of high-dimensional "inverted Keggin" POM materials. The 3D framework belongs to an 8-connected net with the Schläfli symbol of $4^{22}\cdot 6^6$, which is the highest-connected uninodal network topology presently known for POM-based materials. Most strikingly, the 3D compound **1** and 0D compound **2** show photocatalytic activities under visible-light irradiation. The presence of $[Mo_{12}O_{46}(AsPh)_4]^{4-}$ species, which can be photoexcited and effectively activate the dye molecules, is responsible for the photocatalytic performance of the two compounds. In addition, compound **1** is photocatalytically more active than compound **2** because of its structural difference in its dimensions.

ASSOCIATED CONTENT

Supporting Information. X-ray crystallographic data in CIF format for **1** and **2**, complementary drawings for crystal structures, structure description of **2**, TG, powder XRD patterns, and tables. This material is available free of charge via the Internet at http://pubs.acs.org.

AUTHOR INFORMATION

Corresponding Author

*E-mail: yangjinnenu@yahoo.com.cn (J.Y.), jianfangma@yahoo.com.cn (J.-F.M.). Fax: +86-431-85098620 (J.-F.M.).

ACKNOWLEDGMENT

We thank the National Natural Science Foundation of China (Grant 21071028, 21001023), the Science Foundation of Jilin Province (20090137, 20100109), the Fundamental Research Funds for the Central Universities, the Specialized Research Fund for the Doctoral Program of Higher Education, the Training Fund of NENU's Scientific Innovation Project, and the Analysis and Testing Foundation of Northeast Normal University for support. We also thank Dr. Shizheng Wen and Prof. Zhongmin Su for the help with DFT calculations and discussions.

REFERENCES

(1) (a) Kozhevnikov, I. V. *Catalysts for Fine Chemical Synthesis-Catalysis by Polyoxometalates*; Wiley: Chichester, U.K., 2002; Vol. 2. (b) Kamata, K.; Sumida, Y.; Yamaguchi, K.; Hikichi, S.; Mizuno, N. *Science* **2003**, *300*, 964. (c) Muller, A.; Shah, S. Q. N.; Bogge, H.; Schmidtmann, M. *Nature* **1999**, *397*, 48. (d) Kuznetsov, A. E.; Geletii, Y. V.; Hill, C. L.; Morokuma, K.; Musaev, D. G. *J. Am. Chem. Soc.* **2009**, *131*, 6844.

(2) (a) Dolbecq, A.; Dumas, E.; Mayer, C. R.; Mialane, P. *Chem. Rev.* **2010**, *110*, 6009. (b) Streb, C.; Ritchie, C.; Long, D. L.; Kögerler, P.; Cronin, L. *Angew. Chem., Int. Ed.* **2007**, *46*, 7579. (c) Zheng, S. T.; Zhang, J.; Yang, G. Y. *Angew. Chem., Int. Ed.* **2008**, *47*, 3909. (d) Yokoyama, A.; Kojima, T.; Ohkubo, K.; Fukuzumi, S. *Chem. Commun.* **2007**, 3997. (e) An, H. Y.; Wang, E. B.; Xiao, D. R.; Li, Y. G.; Su, Z. M.; Xu, L. *Angew. Chem., Int. Ed.* **2006**, *45*, 904. (f) Tian, A. X.; Ying, J.; Peng, J.; Sha, J. Q.; Pang, H. J.; Zhang, P. P.; Chen, Y.; Zhu, M.; Su, Z. M. *Inorg. Chem.* **2009**, *48*, 100. (g) Zhai, Q. G.; Wu, X. Y.; Chen, S. M.; Zhao, Z. G.; Lu, C. Z. *Inorg. Chem.* **2007**, *46*, 5046.

(3) (a) Wang, X. L.; Qin, C.; Wang, E. B.; Su, Z. M. *Chem. Commun.* **2007**, 4245. (b) Jiang, C. J.; Lesbani, A.; Kawamoto, R.; Uchida, S.; Mizuno, N. *J. Am. Chem. Soc.* **2006**, *128*, 14240. (c) Wei, M. L.; He, C.; Hua, W. J.; Duan, C. Y.; Li, S. H.; Meng, Q. J. *J. Am. Chem. Soc.* **2006**, *128*, 13318. (d) Sun, C. Y.; Liu, S. X.; Liang, D. D.; Shao, K. Z.; Ren, Y. H.; Su, Z. M. *J. Am. Chem. Soc.* **2009**, *131*, 1883. (e) Wang, X. L.; Qin, C.; Wang, E. B.; Su, Z. M.; Li, Y. G.; Xu, L. *Angew. Chem., Int. Ed.* **2006**, *45*, 7411.

(4) (a) Sha, J. Q.; Wang, C.; Peng, J.; Chen, J.; Tian, A. X.; Zhang, P. P. *Inorg. Chem. Commun.* **2007**, *10*, 1321. (b) Sha, J. Q.; Peng, J.; Lan, Y. Q.; Su, Z. M.; Pang, H. J.; Tian, A. X.; Zhang, P. P.; Zhu, M. *Inorg. Chem.* **2008**, *47*, 5145. (c) Tian, A. X.; Ying, J.; Peng, J.; Sha, J. Q.; Han, Z. G.; Ma, J. F.; Su, Z. M.; Hu, N. H.; Jia, H. Q. *Inorg. Chem.* **2008**, *47*, 3274. (d) Zhao, X. Y.; Liang, D. L.; Liu, S. X.; Sun, C. Y.; Cao, R. G.; Gao, C. Y.; Ren, Y. H.; Su, Z. M. *Inorg. Chem.* **2008**, *47*, 7133.

(5) (a) An, H. Y.; Xiao, D. R.; Wang, E. B.; Li, Y. G.; Wang, X. L.; Xu, L. *Eur. J. Inorg. Chem.* **2005**, 854. (b) Li, S. Z.; Ma, P. T.; Wang, J. P.; Guo, Y. Y.; Niu, H. Z.; Zhao, J. W.; Niu, J. Y. *CrystEngComm* **2010**, *12*, 1718.

(6) Debray, H. *C. R. Hebd. Seances Acad. Sci.* **1874**, *78*, 1411.

(7) Rosenheim, A.; Traube, A. *Z. Anorg. Chem.* **1915**, *91*, 75.

(8) Barkigia, K. M.; Rajkovic-Blazer, L. M.; Pope, M. T.; Quicksall, C. O. *Inorg. Chem.* **1981**, *20*, 3318.

(9) Nishikawa, T.; Sasaki, Y. *Chem. Lett.* **1975**, 1185.

(10) (a) Burkholder, E.; Wright, S.; Golub, V.; O'Connor, C. J.; Zubieta, J. *Inorg. Chem.* **2003**, *42*, 7460. (b) Burkholder, E.; Zubieta, J. *Inorg. Chim. Acta* **2004**, *357*, 301.

(11) Johnson, B. J. S.; Geers, S. A.; Brennessel, W. W.; Young, V. G. J.; Stein, A. *Dalton Trans.* **2003**, 4678.

(12) Wang, X. L.; Qin, C.; Wang, E. B.; Xu, L.; Su, Z. M.; Hu, C. W. *Angew. Chem., Int. Ed.* **2004**, *43*, 5036.

(13) Albada, G. A. V.; Guijt, R. C.; Haasnoot, J. G.; Lutz, M.; Spek, A. L.; Reedijk, J. *Eur. J. Inorg. Chem.* **2000**, 121.

(14) Sheldrick, G. M. *SHELXS-97, A Program for Automatic Solution of Crystal Structure*; University of Goettingen: Goettingen, Germany, 1997.

(15) Sheldrick, G. M. *SHELXL-97, A Programs for Crystal Structure Refinement*; University of Goettingen: Goettingen, Germany, 1997.

(16) Farrugia, L. J. *WINGX, A Windows Program for Crystal Structure Analysis*; University of Glasgow: Glasgow, U.K., 1988.

(17) (a) Lan, Y. Q.; Li, S. L.; Li, Y. G.; Su, Z. M.; Shao, K. Z.; Wang, X. L. *CrystEngComm* **2008**, *10*, 1129. (b) Qu, X. S.; Xu, L.; Gao, G. G.; Li, F. Y.; Yang, Y. Y. *Inorg. Chem.* **2007**, *46*, 4775. (c) Zheng, Y. Z.; Tong, M. L.; Chen, X. M. *New J. Chem.* **2004**, *28*, 1412.

(18) Brown, I. D.; Altermatt, D. *Acta Crystallogr.* **1985**, *B41*, 244.

(19) (a) Lan, Y. Q.; Li, S. L.; Wang, X. L.; Shao, K. Z.; Su, Z. M.; Wang, E. B. *Inorg. Chem.* **2008**, *47*, 529. (b) Lan, Y. Q.; Li, S. L.; Wang, X. L.; Shao, K. Z.; Du, D. Y.; Zang, H. Y.; Su, Z. M. *Inorg. Chem.* **2008**, *47*, 8179.

(20) (a) Friedrichs, O. D.; O'Keeffe, M.; Yaghi, O. M. *Acta Crystallogr.* **2003**, *A59*, 22. (b) Johnson, B. J. S.; Schroden, R. C.; Zhu, C.; Stein, A. *Inorg. Chem.* **2001**, *40*, 5972.

(21) (a) Zang, H. Y.; Lan, Y. Q.; Yang, G. S.; Wang, X. L.; Shao, K. Z.; Xu, G. J.; Su, Z. M. *CrystEngComm* **2010**, *12*, 434. (b) Zang, H. Y.; Tan, K.; Guan, W.; Li, S. L.; Yang, G. S.; Shao, K. Z.; Yan., L. K.; Su, Z. M. *CrystEngComm* **2010**, *12*, 3684.

(22) (a) Pankove, J. I. *Optical Processes in Semiconductors*; Prentice Hall: Englewood Cliffs, NJ, 1971. (b) Wesley, W. M.; Harry, W. G. H. *Reflectance Spectroscopy*; Wiley: New York, 1966.

(23) (a) Bonchio, M.; Carraro, M.; Scorrano, G.; Bagno, A. *Adv. Synth. Catal.* **2004**, *346*, 648. (b) Chen, C.; Zhao, W.; Lei, P.; Zhao, J.; Serpone, N. *Chem.—Eur. J.* **2004**, *10*, 1956.

(24) Frisch, M. J.; Trucks, G. W.; Schlegel, H. B.; Scuseria, G. E.; Robb, M. A.; Cheeseman, J. R.; Scalmani, G.; Barone, V.; Mennucci, B.; Petersson, G. A.; Nakatsuji, H.; Caricato, M.; Li, X.; Hratchian, H. P.; Izmaylov, A. F.; Bloino, J.; Zheng, G.; Sonnenberg, J. L.; Hada, M.; Ehara, M.; Toyota, K.; Fukuda, R.; Hasegawa, J.; Ishida, M.; Nakajima, T.; Honda, Y.; Kitao, O.; Nakai, H.; Vreven, T.; Montgomery, Jr., J. A.; Peralta, J. E.; Ogliaro, F.; Bearpark, M.; Heyd, J. J.; Brothers, E.; Kudin, K. N.; Staroverov, V. N.; Kobayashi, R.; Normand, J.; Raghavachari, K.; Rendell, A.; Burant, J. C.; Iyengar, S. S.; Tomasi, J.; Cossi, M.; Rega, N.; Millam, N. J.; Klene, M.; Knox, J. E.; Cross, J. B.; Bakken, V.; Adamo, C.; Jaramillo, J.; Gomperts, R.; Stratmann, R. E.; Yazyev, O.; Austin, A. J.; Cammi, R.; Pomelli, C.; Ochterski, J. W.; Martin, R. L.; Morokuma, K.; Zakrzewski, V. G.; Voth, G. A.; Salvador, P.; Dannenberg, J. J.; Dapprich, S.; Daniels, A. D.; Farkas, Ö.; Foresman, J. B.; Ortiz, J. V.; Cioslowski, J.; Fox, D. J. *Gaussian 09*, Revision A02; Gaussian, Inc.: Wallingford, CT, 2009.

(25) (a) Lin, H.; Maggard, P. A. *Inorg. Chem.* **2008**, *47*, 8044. (b) Hu, Y.; Luo, F.; Dong, F. *Chem. Commun.* **2011**, *47*, 761. (c) Wu, Q.; Chen, W. L.; Liu, D.; Liang, C.; Li, Y. G.; Lin, S. W.; Wang, E. *Dalton Trans.* **2011**, *40*, 56.

(26) (a) Guo, Y.; Wang, Y.; Hu, C.; Wang, Y.; Wang, E.; Zhou, Y.; Feng, S. *Chem. Mater.* **2000**, *12*, 3501. (b) Mylonas, A.; Hiskia, A.; Papaconstanitinou, E. *J. Mol. Catal. A: Chem.* **1996**, *114*, 191.

(27) Mylonas, A.; Papacontantinous, E. *J. Photochem. Photobiol. A* **1996**, *94*, 77.

(28) (a) Yu, Z.-T.; Liao, Z.-L.; Jiang, Y.-S.; Li, G.-H.; Chen, J.-S. *Chem.—Eur. J.* **2005**, *11*, 2642. (b) Liao, Z.-L.; Li, G.-D.; Bi, M.-H.; Chen, J.-S. *Inorg. Chem.* **2008**, *47*, 4844.